

Mineralization of osteoblasts with electrospun collagen/hydroxyapatite nanofibers

J. Venugopal · Sharon Low · Aw Tar Choon ·
T. S. Sampath Kumar · S. Ramakrishna

Received: 12 March 2007 / Accepted: 19 September 2007 / Published online: 24 October 2007
© Springer Science+Business Media, LLC 2007

Abstract Regeneration of fractured or diseased bones is the challenge faced by current technologies in tissue engineering. The major solid components of human bone consist of collagen and hydroxyapatite. Collagen (Col) and hydroxyapatite (HA) have potential in mimicking natural extracellular matrix and replacing diseased skeletal bones. More attention has been focused on HA because of its crystallographic structure similar to inorganic compound found in natural bone and extensively investigated due to its excellent biocompatibility, bioactivity and osteoconductivity properties. In the present study, electrospun nanofibrous scaffolds are fabricated with collagen (80 mg/ml) and Col/HA (1:1). The diameter of the collagen nanofibers is around 265 ± 0.64 nm and Col/HA nanofibers are 293 ± 1.45 nm. The crystalline HA (29 ± 7.5 nm) loaded into the collagen nanofibers are embedded within nanofibrous matrix of the scaffolds. Osteoblasts cultured on both scaffolds and show insignificant level of proliferation but mineralization was significantly ($p < 0.001$) increased to 56% in Col/HA nanofibrous scaffolds compared to collagen. Energy dispersive X-ray analysis (EDX) spectroscopy results proved the presence of higher level of calcium and phosphorous in Col/HA nanocomposites than

collagen nanofibrous scaffolds grown osteoblasts. The results of the present study suggested that the designed electrospun nanofibrous scaffold (Col/HA) have potential biomaterial for bone tissue engineering.

1 Introduction

The shortcomings of autografting and allografting; increasing demand of organs and tissues has inspired the scientists for the development of tissue engineering which aims to produce biological substitutes that may overcome the limitations of conventional clinical treatments for damaged tissues or organs [1]. The ideal scaffold should be biocompatible, bioactive, biodegradable, highly porous with a large surface area to volume ratio, mechanically strong and capable of being formed into desired shapes [2]. For bone tissue reconstruction, scaffolds must meet some specific requirements such as high porosity and adequate pore size to facilitate cell seeding and diffusion throughout the whole structure of both cells and nutrients [3]. Biodegradability is essential since the scaffolds need to be absorbed by the surrounding tissues without the necessity of a surgical removal. The rate at which degradation occurs has to coincide as much as possible with the rate of tissue formation; while cells are fabricating their own natural matrix structure around themselves, the scaffold is able to provide structural integrity within the body and eventually it will break down leaving the neotissue [4–6] which will take over the mechanical load [7].

An ideal biomaterial for bone tissue engineering would administer the appropriate signals to direct the process of osteogenesis, such as cell attachment, proliferation, differentiation and mineralization of extracellular matrix [8].

J. Venugopal (✉) · S. Ramakrishna
Nanoscience and Nanotechnology Initiative, Division of
Bioengineering, National University of Singapore, Block E3,
#05-14, 9 Engineering Drive 1, Singapore 117576, Singapore
e-mail: engjrv@nus.edu.sg

S. Low · A. T. Choon
StemLife Sdn Bhd, Kuala Lumpur 50450, Malaysia

T. S. Sampath Kumar
Department of Metallurgical and Materials Engineering,
Indian Institute of Technology, Chennai, India

It is also based on the idea of a suitable implant material with seeding patients own cells during in vitro culture and prior to transplantation into the defect site, will form a bone tissue [9–11]. Bone tissue contains high levels of type I collagen and several non-collagenous proteins (such as osteopontin, bone sialoprotein and osteocalcin) that distinguish it from other types of tissues [12, 13]. The size of bone mineral is around 50 nm in length, 25 nm in width, and 2–5 nm in thickness [14–16]. These crystals are oriented with their long crystallographic c-axis parallel to each other and aligned with collagen tropocollagen molecules [17, 18]. Collagen is easily degraded and resorbed by the body and allows good attachment to cells. However, its mechanical properties are relatively low ($E \sim 100$ MPa) in comparison to bone ($E \sim 2\text{--}5$ GPa [19]) and it is therefore highly crosslinked or found in composites, such as collagen-glycosaminoglycans for skin regeneration [20] or Col/HA for bone remodeling [21]. Collagen (Col) and hydroxyapatite (HA) devices significantly inhibited the growth of bacterial pathogens, the frequent cause of prosthesis-related infection, compared to PLGA devices [22].

Skeletal bones comprise mainly of collagen (predominantly type I) and carbonate substituted HA, both osteoconductive components. Thus an implant manufactured from such components is likely to behave similarly, and to be of more use than a monolithic device. Indeed, both type I collagen and HA were found to enhance osteoblast differentiation [23] but combined together, they were shown to accelerate osteogenesis. A composite matrix when embedded with human osteoblastic cells showed better osteoconductive properties compared to monolithic HA and produced calcification of identical bone matrix [24, 25]. More interest has been focused to HA because of its crystallographic structure similar to inorganic component found in natural bone. It has been extensively investigated due to its excellent biocompatibility, bioactivity and osteoconductivity [26, 27]. In addition, Col-HA composites proved to be biocompatible both in humans and in animals [28, 29]. Kikuchi et al. fabricated artificial bone material having bone like nanostructure and chemical composition, a composite composed of HA and collagen was synthesized under biomimetic condition through self organization mechanism between HA and collagen [21, 30]. The Col-HA composite fabricated and demonstrated bone like orientation that c-axis of HA nanocrystals were regularly aligned along collagen fibrils [21, 31]. Stable osteoblast cell adhesion is largely mediated by integrins, heterodimeric receptors that interact with extracellular matrix (ECM) proteins, such as fibronectin, vitronectin, fibrinogen and collagen and allows the cell to respond to its extracellular environment as well as to modulate cellular events that regulate remodeling of bone [32, 33]. The aim of this work is to examine the initial response of human osteoblasts to Col/HA nanofibrous

scaffold containing functional groups and mineralization potential to fulfill the criteria of an ideal scaffold for bone tissue engineering.

2 Materials and methods

2.1 Materials

Human fetal osteoblast cells (hFOB) were obtained from the American Type Culture Collection (ATCC, Arlington, VA). Dulbecco's Modified Eagle Medium/Nutrient Mixture F-12 (HAM), fetal bovine serum (FBS), antibiotics and trypsin-EDTA were purchased from GIBCO Invitrogen, USA. CellTiter 96[®] AQueous One solution was purchased from Promega, Madison, WI, USA. Alizarin Red-S and cetylpyridinium chloride purchased from Sigma, St. Louis, MO. Crystalline hydroxyapatite (29 ± 5 nm) was generously provided by the Department of Metallurgical and Materials Engineering, Indian Institute of Technology, Chennai, India.

2.2 Fabrication of Col/HA nanofibers and characterization

Collagen type I (80 mg/ml) was dissolved in 1,1,1,3,3,3-hexafluoro propanol (HFP) under stirring conditions overnight. Col/HA was used 1:1 ratio and dissolved in HFP and stirred for 2 days. The Col/HA nanofibers were fabricated by an electrospinning process, 1.5 ml/h employing an applied voltage of 13 kV using a high voltage power supply (Gamma High Voltage Research, USA). The ground collection plate of aluminum foil was located around 13 cm from the needle tip. A positively charged jet was formed from the Taylor cone and nanofibers were sprayed onto the grounded aluminum foil target. The ambient condition of the spinning apparatus was controlled to be 23 °C and 60% humidity. Cover slips of different sizes were spread on the aluminum foil target to collect nanofibers to investigate biocompatibility by culturing cells as well as to observe the structure and properties of the nanofibers.

These nanofibers were dried under vacuum at room temperature overnight. Electrospun nanofibers were sputter coated with gold (JEOL JFC-1600 Auto Fine Coater, Japan) and visualized by scanning electron microscopy (FEI—OUANTA 200 F, Czech Republic) at an accelerating voltage of 10 kV for characterization. Chemical analysis of Col/HA nanofiber scaffolds were analyzed by Fourier transform infrared (FT-IR) spectroscopy (ThermoNicolet, Avatar 380, USA) over a range between 4,000 and 400 cm^{-1} at 2 cm^{-1} resolution

averaging 100 scans. The crystallite size of HA and morphology were analyzed in a transmission electron microscope (TEM) operated at 120 KeV (JEOL JSM-5600, Japan). TEM specimens were prepared by depositing few drops of HA dispersed in acetone on carbon coated copper grid.

2.3 Human fetal osteoblast cell culture

Human fetal osteoblast cells were cultured in DMEM/F12 medium (1:1) containing 10% FBS in 75 cm² flasks. The osteoblast cultures was maintained at 37 °C in a humidified CO₂ incubator for 6 days and fed every three days and hFOB were harvested from 3rd passage cultures by trypsin EDTA treatment and replated. Populations of cell lines used in this study were between passage 3 and 4.

2.4 MTS assay for hFOB cells proliferation

Human fetal osteoblast cells were seeded (2×10^4 cells/cm²) on collagen, Col/HA nanofibrous scaffolds on 24 well plates. Cell proliferation was monitored after 2, 4 and 6 days by MTS assay (3-(4,5-dimethylthiazol-2-yl)-5-(3-carboxymethoxyphenyl)-2-(4-sulfophenyl)-2H-tetrazolium, inner salt). In order to monitor cell adhesion and proliferation on different substrates, the number of cells was determined by using the colorimetric MTS assay (CellTiter 96[®] AQueous Assay). The mechanism behind this assay is that, metabolically active cells react with a tetrazolium salt in MTS reagent to produce a soluble formazan dye that can be observed at 490 nm. The cellular constructs were rinsed with PBS followed by incubation with 20% MTS reagent in serum free medium for 3 h. Thereafter, aliquots were pipetted into 96 well plates and the samples read in a spectrophotometric plate reader at 490 nm (FLUOstar OPTIMA, BMG Lab Technologies, Germany).

2.5 Processing of hFOB cells for FESEM

Field emission scanning electron microscope (FESEM) was used to monitor cell attachment, morphology and mineral secretion by osteoblasts. hFOB were seeded (2×10^4 cells/cm²) on collagen and Col/HA nanofibrous scaffolds on 24 well plates. After 6 days of the experiment hFOB grown on scaffolds were washed with PBS to remove non-adherent cells and then fixed in 3% glutaraldehyde for 3 h at room temperature, dehydrated through a series of graded alcohol solutions and finally dried in hexamethyldisilazane (HMDS, Sigma) overnight. Dried cellular constructs were sputter coated with gold and

observed under FESEM at an accelerating voltage of 10 kV.

2.6 Energy dispersive X-ray analysis

Surface morphology of materials was studied by using scanning electron microscopy (JEOL–JSM–5500, Germany) at an accelerating voltage of 20 kV and the specimens were coated with gold in an automatic sputter coater. Representative areas of the nanofibrous scaffold surface were observed at the magnification of $\times 200$ and occasionally at higher magnification. Energy dispersive X-ray analysis (EDX) was carried out by using JEOL-EX-23000 BU (Germany) analyzer. The electron beam was used to scan small areas to obtain compositional information from well defined regions of the nanofibrous scaffolds.

2.7 Morphology of human fetal osteoblast cells

Human fetal osteoblasts cultured (2×10^4 cells/cm²) in collagen and Col/HA nanofibrous scaffolds, after 6 days cultures were washed in PBS and stained with a fluorescent molecule, 5-chloromethyl fluorescein diacetate (CMFDA, CellTracker green, Promega USA). Labeling of the cells was performed as described by the manufacturer. The cells were incubated with the dye at a concentration of 5 or 25 μ M. After 60 min of incubation at 37 °C, the CMFDA dye was discarded and the cells were washed with PBS and culture medium added, supplemented with 10% FBS, with the mixture then incubated at 37 °C for an additional 24 h to complete the labeling process. The cells were washed twice with PBS and mounted in the mounting medium. hFOB morphology was observed by Laser Scanning Confocal Microscopy (Leica Microsystems Heidelberg GmbH, Leica TCS SP2, Germany).

2.8 Mineralization of hFOB

Alizarin Red-S (ARS) is a dye which binds selectively calcium salts and widely used for calcium mineral histochemistry. ARS staining was used to detect and quantify mineralization [34]. Nanofibrous scaffolds with hFOB cells (construct) were washed three times in PBS and fixed in ice cold 70% ethanol for 1 h. These constructs were washed three times with dH₂O and stained with ARS (40 mM) for 20 min at room temperature. After several washes with dH₂O, the constructs were observed under optical microscope and the stain was desorbed with the use of 10% cetylpyridinium chloride for 1 h. The dye was collected

and absorbance read at 540 nm in spectrophotometer (Thermo Spectronic).

2.9 Statistical analysis

Experiments were run in the triplicate and repeated at three different times per sample. Differences between two groups were determined by Student *t*-test with values of $p < 0.05$ considered statistically significant.

3 Results

Electrospun nanofibers of collagen and Col/HA were observed and showed interconnected porous structure in Fig. 1 and the fiber diameters are in the range of 265 ± 0.64 and 293 ± 1.45 nm respectively. The crystalline HA (29 ± 7.5 nm) was loaded into the collagen nanofibers and these HA (Fig. 2) were embedded within the nanofibrous matrix of the scaffolds (Fig. 1b). FT-IR spectra showed the typical bands in collagen and Col/HA nanofibers such as N–H stretching at $3,310\text{ cm}^{-1}$ for amide A, C–H stretching at $3,068\text{ cm}^{-1}$ for amide B, C=O stretching at $1,600\text{--}1,700\text{ cm}^{-1}$ for amide I, N–H deformation at $1,500\text{--}1,550\text{ cm}^{-1}$ for amide II and N–H deformation at $1,200\text{--}1,300\text{ cm}^{-1}$ for amide III band (Fig. 3b). Normally, the amide I band is strong, the amide II band is weak and the amide III band is moderate. The amide I, II, and III band regions of the spectrum are directly related to polypeptide conformation.

Data of the conveniently mixed nanocomposite of 50% HA is compared and that of the pure collagen is presented as a reference in Fig. 3a. Along with the amide bands derived from collagen ($\sim 1,650$, $1,550$ and $1,250\text{ cm}^{-1}$), the Col/HA nanocomposite retained additional P–O bands, characterizing poorly crystallized apatite structure. The Col/HA nanocomposite have nonstoichiometric apatite compositions, because the resonance frequencies are close to $1,020\text{ cm}^{-1}$, identified as PO_4^- band nonstoichiometric apatite. We can observe CO_3^- band at 980 cm^{-1} , indicating

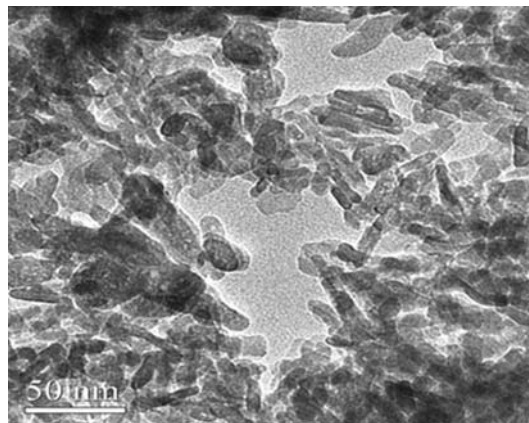


Fig. 2 TEM image of nHA (29 ± 7.5 nm)

the apatite lattice (Fig. 3b). The phosphate band between $1,000\text{ cm}^{-1}$ and $1,150\text{ cm}^{-1}$ indicates the organic-inorganic interaction between crystals and collagen macromolecules had induced nonstoichiometric apatite composition.

The nanocomposites contain amino groups, carboxyl groups and apatite to mimic the natural ECM for hFOB cells to attach, proliferate and migrate inside the nanofibrous scaffolds (Fig. 1b). The cells grew favorably on both nanofibrous scaffolds and the proliferation rate did not increase significantly in collagen compared to Col/HA nanofibrous scaffolds (Fig. 4), the morphology is similar in both nanofibrous scaffolds (Figs. 5, 6). The heterodimeric transmembrane glycoprotein such as integrins present on the cell surface carry negative charges, and the nanofibrous collagen scaffold is positively charged. This opposite polarity would probably accelerate the quick attachment of osteoblasts onto collagen and Col/HA nanofibrous scaffolds, which is a native extracellular matrix protein. Collagen supports the adhesion and proliferation of cells, HA acts as a chelating agent for the mineralization of osteoblasts for bone tissue regeneration.

HA supports the effective affinity for regulating cell function and promoting osteogenesis and mineralization of bone. Cells formed in multilayers and able to observe the mineral particles on the surface of hFOB cells (Fig. 5). Mineralization was significantly ($p < 0.001$) increased to

Fig. 1 FESEM images of electrospun (a) Collagen, (b) Collagen/hydroxyapatite nanofibers

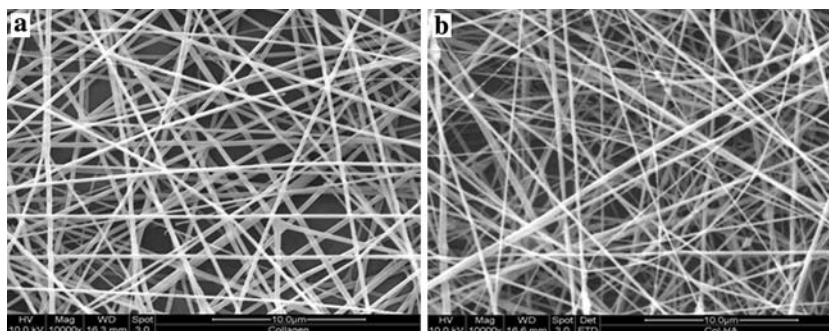


Fig. 3 Fourier transform infrared (FT-IR) spectroscopic analysis of (a) Collagen, (b) Col/HA

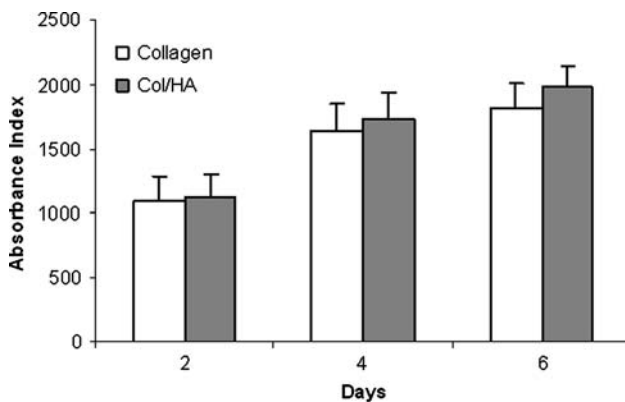
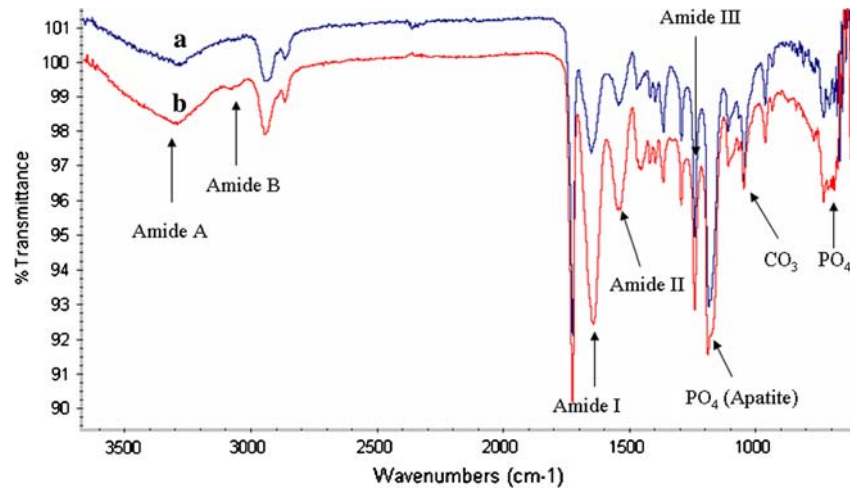
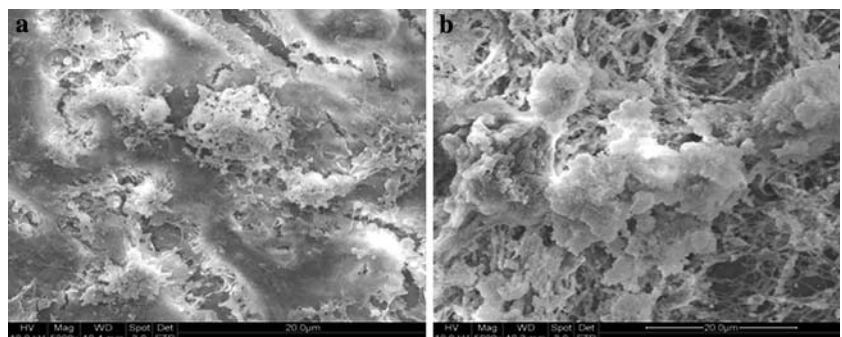


Fig. 4 The hFOB proliferation on collagen and Col/HA nanofibrous scaffolds (*n* = 6). Bar represent means ± SD

56% in Col/HA nanocomposite nanofibrous scaffolds compared to collagen (Fig. 7). The ARS staining also proved increased mineralization after 10 days of osteoblast culture on Col/HA nanofibrous scaffolds (Fig. 8b). EDX spectroscopy results proved the presence of higher level of calcium and phosphorous in Col/HA nanocomposites than collagen nanofibrous scaffolds grown osteoblast cells (Fig. 9). As shown in Fig. 9b peaks of Ca and P were observed as nodules in specific area of osteoblasts on nanofibrous scaffolds.

Fig. 5 FESEM micrographs of hFOB interaction with nanofibrous scaffold after 6 days of culture. (a) Collagen/osteoblasts, (b) Col/HA/osteoblasts



4 Discussion

In biological system, collagen provides space for cell adhesion, differentiation, organogenesis, tissue regeneration and repair. Collagen is mechanically stable with high tensile strength and can be altered into different sizes and shapes with various physical and chemical modifications. The excellent tissue compatibility, decreased antigenicity and biodegradability make collagen as a major resource in biomedical and tissue engineering applications [35]. FESEM images showed proliferation of osteoblasts on both nanofibrous scaffolds and started to fill the spaces after 6 days of culture (Figs. 4, 5). Integrins play a major role in cell attachment and also determine how the cells interpret biochemical signals from their surrounding environment. The $\alpha1\beta1$ and $\alpha2\beta1$ integrins are the major collagen binding integrins, with $\alpha2\beta1$ having higher affinity for fibrillar type I collagen, a major protein constituent of bone. The $\alpha2\beta1$ integrin interaction with type I collagen is crucial signal for the induction of osteoblast differentiation and matrix mineralization [36, 37].

The present study demonstrates the cultured osteoblasts rapidly form an apatite-like, calcium phosphate mineral associated with the cells and their surrounding ECM. The osteoblasts support collagen matrix synthesis and bone

Fig. 6 Morphology of hFOB on nanofibrous scaffolds (CMFDA dye: $\times 10$): (a) Collagen, (b) Col/HA

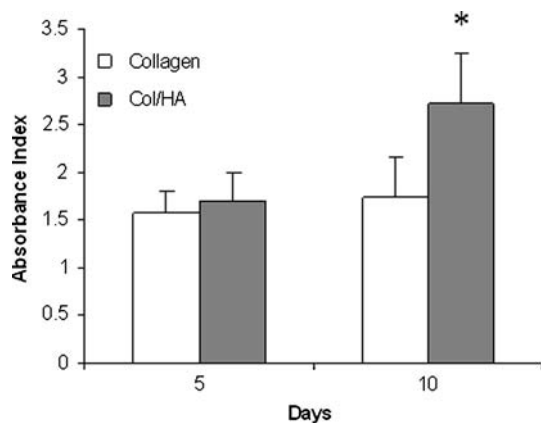
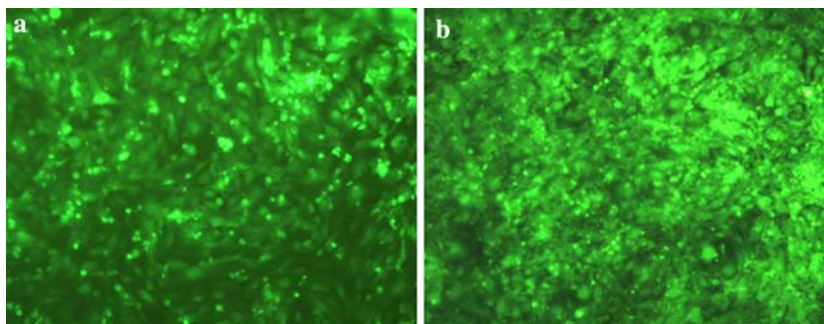
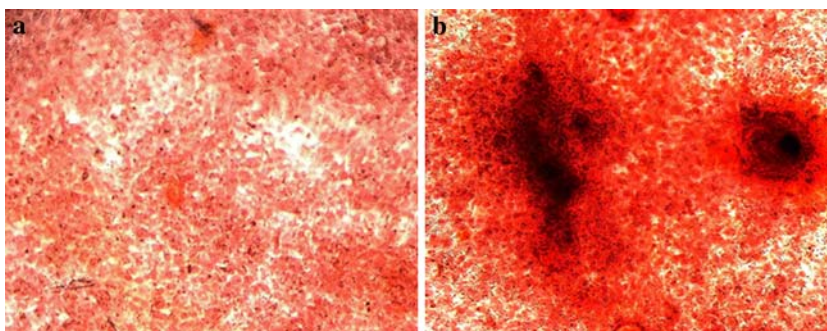


Fig. 7 Alizarin Red-S staining for mineral deposition in hFOB (a) Collagen, (b) Col/HA nanofibrous scaffolds ($*p < 0.001$)

nodule formation on the surface of cells with the activation of HA (Fig. 5). A subsequent period of matrix maturation, collagen synthesis and alkaline phosphatase expressions are elevated and ECM organized in the form of minerals for bone regeneration (Figs. 7, 8). The literature review suggests that the “bone bonding” ability of calcium phosphate ceramics occurs by partial dissolution of ceramic, resulting in elevated concentration of calcium (Ca^{2+}) and phosphate (PO_4^{3-}) ions within the local environment. Investigations have suggested that there is a threshold concentration of calcium ions, required to stimulate the subsequent activity of osteoblasts [38, 39]. The HA/Col composite, designed to simulate bone tissue, is produced using atelocollagen to reduce antigenicity by condensing

Fig. 8 Alizarin Red-S staining for calcium mineralization in hFOB (a) Collagen, (b) Col/HA nanofibrous scaffolds after 10 days of culture



$\text{Ca}(\text{OH})_2/\text{H}_3\text{PO}_4$ suspension [40, 41]. The amount of collagen greatly influenced the nucleation and the development of HA crystalline. The HA/Col composites showed chemical interaction between HA and collagen templates, the COO^- , $\text{C}=\text{O}$, or $-\text{NH}_2$ groups may especially active site for the coordination of calcium ions to form ion complexes as the active sites of nucleation, formation of nuclei of HA is controlled by these special groups. Therefore, the density of charged collagen templates, intensity of interaction between calcium and COO^- , $\text{C}=\text{O}$, amino groups or between amino groups and PO_4^{3-} and accessibility of Ca^{2+} and PO_4^{3-} to collagen network films play very important role in the formation of HA (Fig. 3b). One can control the size of HA through changing the ratio of collagen and Ca^{2+} , PO_4^{3-} to imitate the structure of natural bone.

Calcification occurred at the nucleation site of matrix vesicles present in the lacunae of mineralizing bone. They are believed to accumulate Ca^{2+} and inorganic phosphate, which served as a nucleating agent for the formation of HA, the main organic component of bone (Fig. 5b). In the case of metabolic (cell-mediated) calcification, deposition of salts has to be preceded by the formation of an inorganic extracellular compartment [42]. To be representative for bone formation, mineralization must be osteoblast mediated: a collagen type I containing extracellular compartment has to be formed, on which, via extrusion of membrane-bound vesicles loaded with crystals, mineralization was formed on the surface of cells. EDX results indicated that the cells are able to attach and grow on

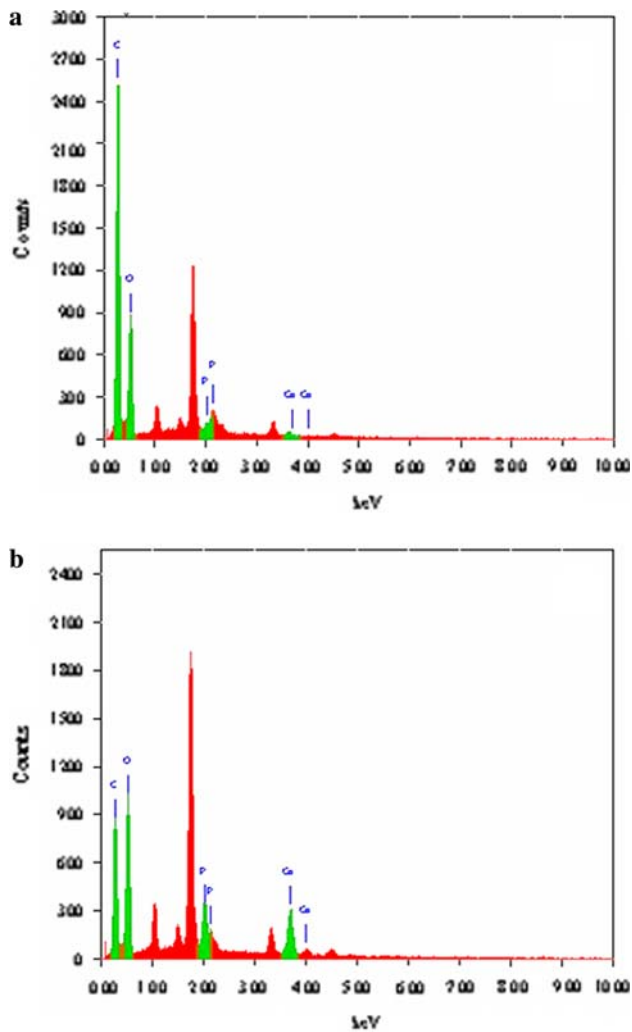


Fig. 9 EDX analysis for the detection of mineralization after 6 days of hFOB culture (**a**) Collagen nanofibrous scaffold, (**b**) EDX detected significantly higher levels of phosphorus and calcium in Col/HA nanofibrous scaffolds

collagen nanofibrous scaffolds in the presence of HA to form mineralized tissue, which primarily consists of calcium and phosphorous deposits (Fig. 9b). These results were further supported by qualitative and quantitative analysis of ARS-calcium expression, with the highest calcium concentration measured on Col/HA nanofibrous scaffolds (Figs. 7, 8).

Morphological evidence demonstrated large number of extracellular mineral deposits on the basal surface of cells that contained crystalline structures associated with a fibrous organic matrix; relatively lot of mineral deposits were detected on the surface of osteoblast cells. Figure 7 showed mineralization of osteoblasts increased significantly ($p < 0.001$) in composite nanofibrous scaffold (Col/HA) compared to collagen and the mineral particles are stained with ARS dye (Fig. 8). The mineral deposition in cultured osteoblasts was significantly increased in

composite nanofibrous scaffolds than collagen nanofibrous scaffolds during 10 days of culture period. In Col/HA composite nanofibrous scaffolds without HA, mineral deposition was significantly lower upto 56% than in collagen nanofibrous scaffolds. Based on these results, the Col/HA composite nanofibrous scaffold developed in this study is considered as a potential biomaterial for the adhesion and growth, as well as to stimulate them for mineralization to exhibit functional activity of osteoblasts for bone tissue engineering.

5 Conclusion

The interconnecting porous structure of the composite nanofibrous scaffolds (Col/HA) provide more structural space for the adhesion, accommodation, proliferation and mineralization of osteoblasts and enable the efficient exchange of nutrients and metabolic waste. Osteoblasts cultured on composite nanofibrous scaffold showed normal rate of proliferation, higher level of mineralization and moderate increase in calcium and phosphorous activity through the activation of HA and forming multilayer of cells for the construction of natural bone tissue. Based on these studies, electrospun Col/HA composite nanofibrous scaffold hold great potential for the mineralization of osteoblasts and considered as a promising biomaterial for bone tissue regeneration.

Acknowledgements This study was supported by Office of Life Sciences in National University of Singapore and StemLife Sdn Bhd, 50450 Kulalumpur, Malaysia.

References

1. X. LI and J. CHANG, *J. Mater. Sci. Mater. Med.* **16** (2005) 365
2. Y. ZHANG and M. Q. ZHANG, *J. Biomed. Mater. Res.* **61** (2002) 1
3. S. H. HSU, H. J. YEN, C. S. TSENG, C. S. CHENG and C. L. TSAI, *J. Biomed. Mater. Res.* **80** (2007) 519
4. L. E. FREED, J. C. MARQUIS, A. NOHRIA, J. EMMANUAL and A. G. MIKOS, *J. Biomed. Mater. Res.* **27** (1993) 11
5. D. A. GRAND, C. HALBERSTADT, G. NAUGHTON, R. SCHWARTZ and R. MANJI, *J. Biomed. Mater. Res.* **34** (1997) 211
6. G. A. AMEER, T. A. MAHMOOD and R. A. LANGER, *J. Orthop. Res.* **20** (2002) 16
7. http://en.wikipedia.org/wiki/Tissue_engineering
8. J. R. JONES, O. TSIGKOU, E. E. COATES, M. M. STEVENS, J. M. POLAK and L. L. HENCH, *Biomaterials* **28** (2007) 1653
9. S. C. MENDES, J. M. TIBBE, M. VEENHOF, S. BOTH and J. D. DE BRUIJN, *J. Mater. Sci. Mater. Med.* **15** (2004) 1123
10. S. C. MENDOS, J. D. DE BRUIJN, A. A. APELDOORN, P. P. PLATENBURG, G. J. M. TIBBE and C. A. VAN BLITTERWIJK in “Bone Engineering”, edited by J. E. Davies (Em Square Incorporated, Toronto, 2000) p. 505
11. J. D. DE BRUIJN and C. A. VAN BLITTERSWIJK in “Biomaterials in Surgery” edited by G. H. J. M. Walenkamp (Stuttgart, 1998) p. 77

12. M. WEINREB, D. SHINAR and G. RODAN, *ibid.* **5** (1990) 831
13. P. DERKX, A. L. NIGG, F. T. BOSMAN, A. P. POLS and T. M. VAN LEEUWEN, *ibid.* **22** (1998) 367
14. R. A. ROBINSON, *J. Bone Joint Surg. Am.* **34A** (1952) 389
15. E. JOHANSEN and H. F. PARKS, *J. Biophys. Biochem. Cytol.* **7** (1960) 743
16. E. SACHLOS, D. GOTORA and J. T. CZERNUSZKA, *Tissue Eng.* **12** (2006) 2479
17. S. WEINER and W. TRAUB, *Tissue Res.* **21** (1989) 589
18. W. J. LANDIS, M. J. SONG, A. LEITH, L. McEWEN and B. F. McEWEN, *J. Struct. Biol.* **110** (1993) 39
19. K. I. CLARKE, S. E. GRAVES, A. T. C. WONG, J. T. TRIFFIT, M. J. O. FRANCIS and J. T. CZERNUSZKA, *J. Mater. Sci. Mater. Med.* **4** (1993) 107
20. F. J. O'BRIEN, B. A. HARLEY, I. V. YANNAS and L. GIBSON, *Biomaterials* **25** (2004) 1077
21. M. KIKUCHI, H. N. MATSUMOTO, T. YAMADA and J. TANAKA, *Biomaterials* **25** (2004) 63
22. G. A. CARLSON, J. L. DRAGOO, B. SAMIMI, D. A. BRUCKNER and P. BENHAIM, *Biochem. Biophys. Res. Commun.* **321** (2004) 472
23. J. XIE, M. J. BAUMANN and L. R. McCABE, *J. Biomed. Mater. Res.* **71A** (2004) 108
24. C. M. SERRE, M. M. PAPILLARD, P. CHAVASSIEUX and G. BOIVIN, *Biomaterials* **14** (1993) 97
25. M. L. WANG, R. TULI, P. A. MANNER, D. J. HALL and R. S. TUAN, *J. Mater. Sci. Lett.* **14** (1995) 490
26. J. LI, Y. CHEN, Y. YIN, F. YAO and K. YAO, *Biomaterials* **28** (2007) 781
27. R. MURUGAN and S. RAMAKRISHNA, *Biochem. Biophys. Res.* **292** (2002) 1
28. A. SCABBIA and L. TROMBELLI, *J. Clin. Periodontol.* **31** (2004) 348
29. D. WAHL and T. J. CZERNUSZKA, *Euro. Cells Mater.* **11** (2006) 43
30. G. GRONOWICZ and M. B. McCARTHY, *J. Orthop. Res.* **14** (1996) 878
31. K. M. WOO, V. J. CHEN and P. X. MA, *J. Biomed. Mater. Res.* **67A**, 531 (2003)
32. L. GRIFFITH, *Acta Mater.* **48** (2000) 263
33. R. LANGER and D. A. TRILL, *Nature* **428** (2004) 487
34. C. A. GREGORY, W. G. GUNN, A. PEISTER and D. J. PROCKOP, *Anal. Biochem.* **329** (2004) 77
35. J. GEORGE, Y. KUBOKI and T. MIYATA, *Biotechnol. Bioeng.* **95**, 405 (2006)
36. M. MIZUNO, R. FUJISAWA and Y. KUBOKI, *J. Cell Physiol.* **184** (2000) 207
37. M. MIZUNO and Y. KUBOKI, *J. Biochem (Tokyo)*. **129** (2001) 129
38. J. GLOWACHI, D. ALTOBELLI and A. J. MULLIKEN, *Calcif. Tiss. Int.* **33** (1981) 71
39. A. PORTER, N. PATEL, R. BROOKS and W. BONFIELD, *J. Mater. Sci. Mater. Med.* **16** (2005) 899
40. S. ITOH, M. KIKUCHI and K. TAKAKUDA, *J. Biomed. Mater. Res.* **63** (2002) 507
41. T. NISHIKAWA, K. MASUNO, K. TOMINAGA and A. TANAKA, *Implant. Dent.* **14** (2005) 252
42. A. L. BOSKEY, *Conn. Tissue Res.* **35** (1996) 35